

Article

## The Reaction of Thiyl Radical with Methyl Linoleate: Completing the Picture

Chryssostomos Chatgililoglu, Carla Ferreri, Maurizio Guerra, Abdelouahid Samadi, and Vincent William Bowry

*J. Am. Chem. Soc.*, **Just Accepted Manuscript** • DOI: 10.1021/jacs.6b11320 • Publication Date (Web): 02 Mar 2017

Downloaded from <http://pubs.acs.org> on March 3, 2017

### Just Accepted

“Just Accepted” manuscripts have been peer-reviewed and accepted for publication. They are posted online prior to technical editing, formatting for publication and author proofing. The American Chemical Society provides “Just Accepted” as a free service to the research community to expedite the dissemination of scientific material as soon as possible after acceptance. “Just Accepted” manuscripts appear in full in PDF format accompanied by an HTML abstract. “Just Accepted” manuscripts have been fully peer reviewed, but should not be considered the official version of record. They are accessible to all readers and citable by the Digital Object Identifier (DOI®). “Just Accepted” is an optional service offered to authors. Therefore, the “Just Accepted” Web site may not include all articles that will be published in the journal. After a manuscript is technically edited and formatted, it will be removed from the “Just Accepted” Web site and published as an ASAP article. Note that technical editing may introduce minor changes to the manuscript text and/or graphics which could affect content, and all legal disclaimers and ethical guidelines that apply to the journal pertain. ACS cannot be held responsible for errors or consequences arising from the use of information contained in these “Just Accepted” manuscripts.

1  
2  
3  
4 The Reaction of Thiyl Radical with Methyl Linoleate:  
5  
6

7  
8 Completing the Picture  
9

10  
11 *Chryssostomos Chatgililoglu,\* † Carla Ferreri, † Maurizio Guerra, †,§ Abdelouahid Samadi# and*  
12

13  
14 *Vincent W. Bowry‡*  
15

16  
17 **Corresponding Author**  
18

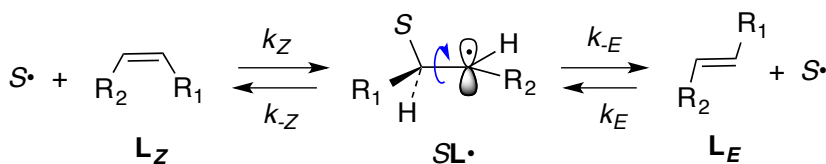
19 [chrys@isof.cnr.it](mailto:chrys@isof.cnr.it)  
20  
21  
22  
23  
24  
25  
26  
27  
28  
29  
30  
31  
32  
33  
34  
35  
36  
37  
38  
39  
40  
41  
42  
43  
44  
45  
46  
47  
48  
49  
50  
51  
52  
53  
54  
55  
56  
57  
58  
59  
60

1  
2  
3  
4 ABSTRACT: *Cis* lipids can be converted by thiols and free radicals into *trans* lipids, which are  
5  
6 therefore a valuable tell-tale for free radical activity in the cell's lipidome. Our previous studies  
7  
8 have shown that polyunsaturated lipids are isomerized by alkanethiyl radicals ( $S^\bullet$ ) in a cycle  
9  
10 propagated by reversible double-bond addition and terminated by radical H-abstraction from the  
11  
12 lipid. A critical flaw in this picture has long been that the reported lipid abstraction rate from  
13  
14 radiolysis studies is faster than addition-isomerization, *implying that the "cycle" must be*  
15  
16 *terminating faster than it is propagating!* Herein, we resolved this longstanding puzzle by  
17  
18 combining a detailed product analysis, with reinvestigation of the time-resolved kinetics, DFT  
19  
20 calculations of the indicated pathways, and reformulation of the radical-stasis equations. We  
21  
22 have determined thiol-coupled products in dilute solutions arise mainly from addition to the  
23  
24 inside position of the bisallylic group, followed by *rapid* intramolecular H•-transfer, yielding  
25  
26 allylic radicals ( $L_{ZZ} + S^\bullet \rightleftharpoons SL^\bullet \rightarrow SL'^\bullet$ ) that are *slowly* reduced by thiol ( $SL'^\bullet + SH \rightarrow SL'H +$   
27  
28  $S^\bullet$ ). The first-order grow-in rate of  $L_{H}^\bullet$  signal ( $k_{\text{exp}}^{280\text{nm}}$ ) may therefore be dominated by the  
29  
30 addition-H-translocation rather than slower direct H•-abstraction. Steady-state kinetic analysis of  
31  
32 the new mechanism is consistent with products and the rates and trends for polyunsaturated fatty  
33  
34 acids (PUFAs), monounsaturated fatty acids (MUFAs) and mixtures, with and without  
35  
36 physiological  $[O_2]$ . Implications of this new paradigm for the thiol-ene reactivity fall in an  
37  
38 interdisciplinary research area spanning from synthetic applications to metabolomics.  
39  
40  
41  
42  
43  
44  
45  
46  
47  
48  
49  
50  
51  
52  
53  
54  
55  
56  
57  
58  
59  
60

## INTRODUCTION

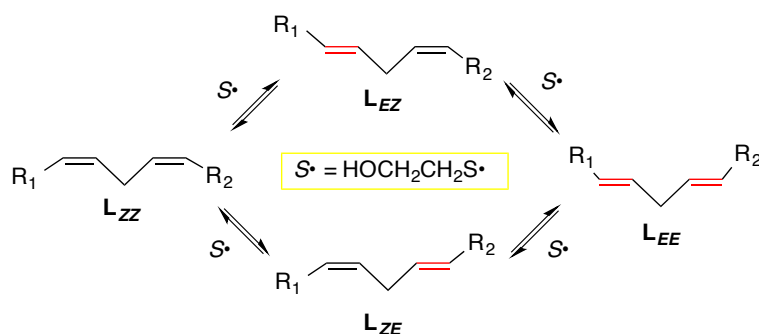
Free radical-catalyzed cis-trans isomerization of unsaturated lipids in biomimetic conditions<sup>1,2</sup> has been a subject of interest in our laboratory for the last decade. We provided indications for an endogenous origin of trans unsaturated fatty acids in cells,<sup>3</sup> animals<sup>4</sup> and humans<sup>5,6</sup> based on mono-trans PUFA isomers as biomarkers.<sup>7</sup> We embarked on a study of tandem protein-lipid damages under radical stress and discovered that sulfur-containing proteins can produce diffusible thiyl radicals able to induce cis-trans isomerization in unsaturated lipid vesicles.<sup>8,9</sup> We have identified this chemical reactivity leading to Met-enkephalin,<sup>10</sup> amyloid,<sup>11</sup> bovine RNase A,<sup>12,13</sup> human serum albumin<sup>14</sup> and various metalloproteins.<sup>15</sup>

### Scheme 1. Thiyl catalyzed isomerization of a lipid double bond



Some years ago we investigated the kinetics of the cis-trans (*Z-E*) isomerization of methyl oleate catalyzed by thiyl radicals.<sup>16-19</sup> Double-bond isomerization occurs via the addition-rotation-fragmentation cycle of Scheme 1 (where the thiyl S• is derived from SH = HOCH<sub>2</sub>CH<sub>2</sub>SH or other organic thiol). The progress rate data yielded cis and trans addition rate constants  $k_Z = 1.6 \times 10^5$  and  $k_E = 2.9 \times 10^5 \text{ M}^{-1} \text{ s}^{-1}$  and fragmentation rate constants  $k_{-Z} = 1.6 \times 10^7$  and  $k_{-E} = 1.4 \times 10^8 \text{ s}^{-1}$ .

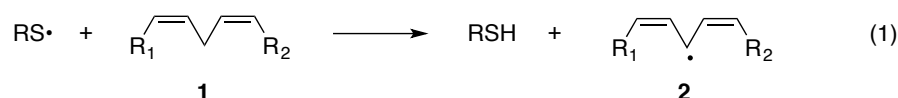
While methyl oleate isomerization appeared<sup>20</sup> to be well understood,<sup>21</sup> at no stage could the same be said for the analogous reaction of the linoleate and other PUFA species. The time profiles for disappearance of linoleic acid (9cis,12cis-C18:2) methyl ester (L<sub>ZZ</sub>) and formation of mono-trans and di-trans isomers (L<sub>EZ</sub>, L<sub>ZE</sub> and L<sub>EE</sub>) in these experiments showed that the isomerization occurs stepwise (Scheme 2).<sup>1,2a,7</sup>

**Scheme 2.** Stepwise isomerization of linoleic acid methyl ester

However, side reactions are also clearly at work. In particular, bisallylic H-abstraction (below) afforded byproducts containing *conjugated diene* moieties that would be inhibitors for the cis-trans isomerization catalytic cycle.<sup>19</sup> We also found that the corresponding inhibition in the isomerization of soybean or egg lecithins in organized systems like large unilamellar vesicles (LUV) was regioselective and less defined by the lipid class.<sup>7,19</sup> It is worth mentioning that the interplay of lipid peroxidation and cis-trans isomerization occurring in linoleic acid micelles in the presence of oxygen and thiols has been reported. It was demonstrated that conjugated diene hydroperoxides and mono-trans isomers are formed to comparable extent.<sup>22</sup> It is also worth noting that the unsaturated lipid-thiol reactions and their radical-induced cross-linked products occupy a wide interdisciplinary research area spanning from synthetic and material applications to biology and metabolomics. In fact, PUFA-thiol adducts were observed in vivo formed by CCl<sub>4</sub> toxicity and impair the enzymatic repair, that seems to work better when oxidative lipid lesions are formed.<sup>23</sup> On the other hand, unsaturated lipids are growingly used as “green” substrates for preparative thiol-ene coupling (TEC) reactions.<sup>24</sup> The photo-reactions of corn and canola oils with butane-thiol, e.g.,<sup>24a</sup> and dye-containing thiols<sup>24c</sup> have been reported, and so has the reaction of a poly-thiol with pure MUFA and PUFA methyl esters.<sup>25</sup> In the latter study the PUFA esters reacted far slower than did the MUFA esters; in both studies the TEC reactions

1  
2  
3 produced no NMR-detectable conjugated moieties. This would seem at odds with the idea of  
4  
5 *product inhibition*; that it is the conjugated products from PUFAs that slow their reactions with  
6  
7 the thiol. The source of the rate-retarding effect of PUFAs in the thiol photo-reaction with mixed  
8  
9 lipids (e.g., edible oils) has therefore remained a moot point.  
10  
11

12 Serious difficulties arise when the kinetics of the (known) side-reactions in the chain or cycle  
13  
14 are examined. PUFA lipids (**1**) have methylene-interrupted double bonds, and the bisallylic  
15  
16 positions have quite a low C-H bond dissociation enthalpy, so that the reaction with alkanethiyl  
17  
18 radicals ( $S^\bullet = RS^\bullet$ ) is strongly exothermic (eq 1,  $\Delta H_{(1)} \approx -11$  kcal/mol) and hence irreversible.  
19  
20



27 In 1989, two independent groups reported on the reaction of cysteinyl ( $CyS^\bullet$ )<sup>26</sup> and  
28  
29 glutathionyl ( $GS^\bullet$ )<sup>27</sup> radicals with PUFA esters. Both groups found rate constants faster than  $k_1$   
30  
31  $\sim 10^7 \text{ M}^{-1}\text{s}^{-1}$  for Reaction 1 based on pulse radiolysis methods. Willson and co-workers<sup>27</sup> reported  
32  
33 on the competition between Reaction 1 and the reaction of  $GS^\bullet$  with probe molecule ABTS,  
34  
35 whereas Asmus and coworkers described the direct formation of pentadienyl radical **2** by the  
36  
37 action of ( $S^\bullet =$ )  $CyS^\bullet$  radical. The reported rate constants increased in the series linoleic <  $\alpha$ -  
38  
39 linolenic < arachidonic (i.e., mirroring the numbers of bisallylic groups).<sup>26</sup> In 1992, Schöneich et  
40  
41 al. reported a detailed study of the reaction of PUFA with a variety of thiyl radicals by pulse  
42  
43 radiolysis techniques, where these findings were confirmed and extended.<sup>28</sup> Relevant to the  
44  
45 present work is the rate constant of  $3.1 \times 10^7 \text{ M}^{-1}\text{s}^{-1}$  for the reaction of  $HO(CH_2)_2S^\bullet$  radical with  
46  
47 linoleic acid. On the basis of several assumptions, mechanistic proposals were advanced.<sup>29</sup> For  
48  
49 example, it was proposed that: (i)  $\sim 50\%$  of thiyl radicals abstract the bisallylic hydrogen,  
50  
51 whereas the remaining  $RS^\bullet$  add to the double bond to form a radical adduct, and (ii) the presence  
52  
53 of molecular oxygen efficiently scavenges all the formed carbon-centered radicals.<sup>29</sup> Whereas,  
54  
55  
56  
57  
58  
59  
60

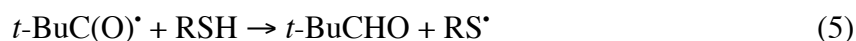
1  
2  
3 contrary to (i), the reaction propagates in a chain, with 15 or more trans bonds being formed in  
4  
5 PUFA lipid per initiating radical and, contrary to (ii), ( $S\bullet =$ )  $\text{HO}(\text{CH}_2)_2\text{S}\bullet$  induced cis-trans  
6  
7 isomerizations of methyl oleate or methyl linoleate in *tert*-butanol solutions are hardly affected  
8  
9  
10 by oxygen concentrations lower than 0.3 mM.  
11

12  
13 Thus, as we have previously pointed out,<sup>1a,2a</sup> there are critical contradictions between time-  
14  
15 resolved data (for eq 1) and product data, as there are inconsistencies between data for the  
16  
17 MUFA and PUFA esters. Herein, we investigated the kinetics of the linoleate-thiyl radical  
18  
19 reaction by carefully matching and comparing laser flash photolysis (LFP) reaction rate data with  
20  
21 a detailed product analysis. Our findings – in conjunction with DFT analysis of the reaction steps  
22  
23 and a ground-up remodeling of the radical-chain kinetics – reveal unheralded mechanisms that  
24  
25 resolve these long-standing issues with lipid-thiol reactions.  
26  
27

## 28 29 30 **RESULTS AND DISCUSSION**

31  
32 **Product Studies.** As previously,<sup>18</sup> thiyl radicals were selectively generated by photolysis of di-  
33  
34 *tert*-butyl ketone ( $t\text{-Bu}_2\text{CO}$ ) and  $\beta$ -mercaptoethanol ( $\text{RSH}$ ,  $\text{R} = \text{HO}(\text{CH}_2)_2\text{-}$ ) in de-aerated  
35  
36 alcoholic solutions that, in the absence of lipid, afforded only the corresponding disulfide ( $(\text{RS})_2$ ,  
37  
38 eq 6). Light is absorbed by the ketone leading to classical Type I cleavage from the ketone triplet  
39  
40 state (eq 2) with a quantum yield  $\Phi = 0.72$  which was independent of the solvent. The rate  
41  
42 constant for subsequent decarbonylation of the acyl radical (eq 3) is solvent dependent and close  
43  
44 to  $5 \times 10^5 \text{ s}^{-1}$  for alcoholic solutions. The radicals formed by the photolysis abstract hydrogen  
45  
46 atoms from the thiol faster than they terminate, congruent with the fact that both alkyl and acyl  
47  
48 radicals react with alkane-thiol with rate constants close to  $10^7 \text{ M}^{-1} \text{ s}^{-1}$  (eqs 4 and 5).<sup>30</sup> Solutions  
49  
50 containing 27.5 mM  $t\text{-Bu}_2\text{CO}$  were estimated have a steady-state concentration of thiyl radicals  
51  
52  
53  
54  
55  
56  
57  
58  
59  
60

[RS•] = 12 nM. Samples in a quartz photochemical reactor were exposed to UV irradiation (240–350 nm) using a low-pressure mercury lamp and a Kasha filter at pH 1.



With higher thiol concentrations in *tert*-butyl or isopropyl alcohol {containing  $\mathbf{L}_{ZZ}$  (150 mM), *t*-Bu<sub>2</sub>CO (37.5 mM), and HO(CH<sub>2</sub>)<sub>2</sub>SH ( $\geq 75$  mM)} the results were similar to our previous observations;<sup>18</sup> viz., slow step-by-step isomerization (as per Scheme 2) and minor consumption of the sum of all geometrical isomers. Next we proceeded by mapping the reaction outcome for lower concentrations: i.e., after 15 min photolysis using different thiol concentrations (7, 15, 25, 50, 75 mM) for each  $\mathbf{L}_{ZZ}$  concentration (15, 30, 50, 100 mM).<sup>31</sup> The rate of the isomerization increased with decreasing  $\mathbf{L}_{ZZ}$  concentrations or with increasing thiol concentration. At increased thiol concentration, side reactions occurred at greater extent, e.g., the reaction of 15 mM  $\mathbf{L}_{ZZ}$  with 7 or 75 mM thiol showed side reactivity other than fatty acid isomerization of 54% or 90%, respectively. On the other hand, by keeping the same amount of thiol (50 mM) in the reaction with 15 or 100 mM  $\mathbf{L}_{ZZ}$  lead to 80% or 5% side reactivity, respectively.

Two sets of experimental conditions were chosen for determining the reaction time profile.

Figure 1 (upper side) displays the development of the isomer concentrations as a function of the reaction time, using 50 mM  $\mathbf{L}_{ZZ}$  and 20 mM HO(CH<sub>2</sub>)<sub>2</sub>SH. The loss of  $\mathbf{L}_{ZZ}$  was matched by the formation of mono- and all-trans isomers ( $\mathbf{L}_{ZE}$ ,  $\mathbf{L}_{EZ}$  and  $\mathbf{L}_{EE}$ ). The two mono-trans isomers were found in equal amounts and are reported together. The equilibrium of the various geometrical

isomers was reached at  $\sim 1300$  s of irradiation in the statistical ratio  $L_{ZZ}:L_{ZE}:L_{EZ}:L_{EE} = 4/13/13/70$ . Whereas, the sum of all geometrical isomers decreased with increasing reaction time, indicating other products are formed to account for the full mass balance. Fig. 1 (lower side) shows there is a higher loss of unsaturation for a ten-fold decrease of methyl linoleate ( $L_{ZZ}$ ) concentration. Under these conditions, the relative rate of cis-trans isomerization increased and the various geometrical isomers reached their equilibrium at  $\sim 100$  s of irradiation.

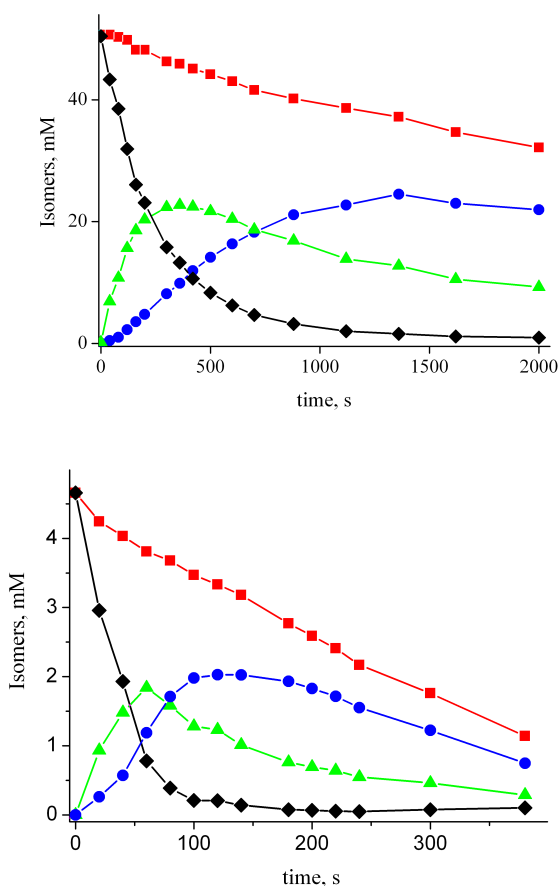


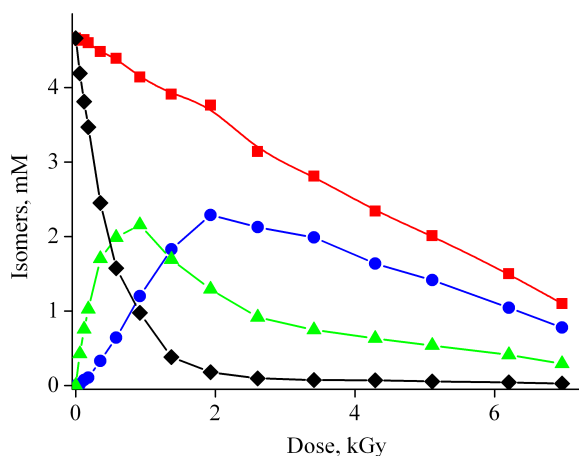
**Figure 1.** Time profile of cis-trans isomerization of methyl linoleate (upper:  $[L_{ZZ}]_0 = 50$  mM; lower: 4.7 mM) catalyzed by thiyl radicals generated by photolysis of *t*-Bu<sub>2</sub>CO (37.5 mM) and HO(CH<sub>2</sub>)<sub>2</sub>SH (20 mM) in isopropanol at  $20 \pm 1$  °C. Profiles: (◆)  $L_{ZZ}$ , (▲)  $L_{ZE}$  and  $L_{ZE}$ , (●)  $L_{EE}$ , and (■) sum of all geometrical isomers, i.e.,  $L_{ZZ}+L_{ZE}+L_{EZ}+L_{EE}$ .

$\gamma$ -Radiolysis gave comparable results. Thus,  $\gamma$ -radiolysis of  $N_2O$ -saturated isopropanol led to the transient species shown in eqs 7-9,



where  $R' \cdot$  represent the produced carbon-centered radicals. In particular, solvated electrons are efficiently quenched by  $N_2O$  to give  $O^-$  (eq 8,  $k_8 = 9.1 \times 10^9 \text{ M}^{-1} \text{ s}^{-1}$ ).<sup>32</sup> Hydrogen abstraction from isopropanol by  $O^-$  radical increased the production of alkyl radical species (eq 9,  $k_9 = 1.2 \times 10^9 \text{ M}^{-1} \text{ s}^{-1}$ ). All  $R''$  radicals reacted with thiol to give the corresponding thiyl radical (eq 10).<sup>32</sup>

Figure 2 (upper side) displays the development of the isomer concentrations as a function of the reaction time for 4.7 mM  $L_{ZZ}$  and 20 mM RSH from the radiolysis experiments. It is gratifying to see the similarity of this figure with the analogous photolysis experiment (lower side of Fig. 1).



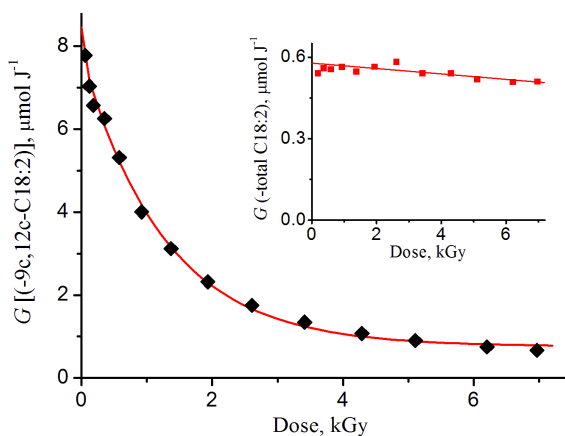


**Figure 2.** (Upper) Dose profile of cis-trans isomerisation of methyl linoleate (4.7 mM) catalyzed by thiyl radicals generated by  $\gamma$ -radiolysis of  $\text{HO}(\text{CH}_2)_2\text{SH}$  (20 mM) in  $\text{N}_2\text{O}$ -saturated isopropanol at 22 °C; Profiles: ( $\blacklozenge$ )  $L_{ZZ}$ , ( $\blacktriangle$ )  $L_{ZE}$  and  $L_{ZE}$ , ( $\bullet$ )  $L_{EE}$ , and ( $\blacksquare$ ) sum of all geometrical isomers, i.e.,  $L_{ZZ}+L_{ZE}+L_{EZ}+L_{EE}$ . (Lower) The chemical radiation yields ( $G$ ) of disappearance of  $L_{ZZ}$  versus dose; the inset shows the  $G$  for the consumption of all geometrical isomers (total  $L$ ) as a function of the irradiation dose.

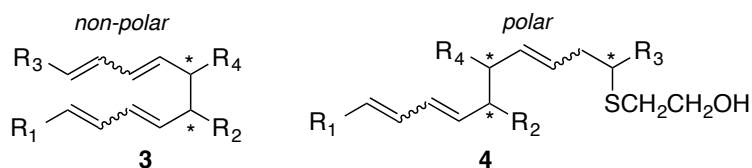
The disappearance of the starting material (mol/kg) divided by the absorbed dose ( $1\text{Gy} = 1\text{ J/kg}$ ) gives the radiation chemical yield or  $G[-L_{ZZ}]$ . Fig. 2 (lower side) shows the plot of  $G[-L_{ZZ}]$  versus dose. The extrapolation to zero dose gives  $G = 8.2\ \mu\text{mol/J}$ . Assuming that the  $G(\text{RS}\cdot)$  is  $0.65\ \mu\text{mol}$ ,<sup>33</sup> we calculated the catalytic cycle (or chain length) to be 13 at the initial phase. For the analogous isomerization of 0.15 M methyl linoleate and 75mM SH, a catalytic cycle of 14 was calculated.<sup>19</sup> While the  $G$  for disappearance of the sum of geometrical isomers is  $0.58\ \mu\text{mol/J}$  (lower Fig. 2 inset), which suggests that each thiyl radical consumes one molecule of  $L_{ZZ}$  or its geometrical isomers (total  $L$ ). A previous product study of thiyl radical-catalyzed isomerization of linoleic acid methyl ester by  $\gamma$ -irradiation showed 0.15M  $L_{ZZ}$  and 0.075M  $\text{HO}(\text{CH}_2)_2\text{SH}$  in *t*-BuOH affording the cis/trans isomer mixture (93% yield) as the main reaction products, accompanied by a 4% yield of dimeric conjugated derivatives **3** and 2% of a mixture of thiol-

1  
2  
3 linoleate adducts.<sup>19</sup> In summary, then, the cycle number for the loss of lipid (to dimers and  
4  
5  
6 adducts) was  $\sim 1.0$  (indicating first-order termination), while the cycle number for the loss of cis-  
7  
8  
9 double bonds in the lipid was  $\sim 14$ , i.e., independent of the lipid concentration but dependent on  
10  
11 [thiol] in dilute solutions.

12  
13 In the present study, careful isolation and detailed characterization of the reaction products  
14  
15 were carried out after the reaction of 4.6 mM methyl linoleate ( $L_{ZZ}$ ) with 20 mM  $\text{HO}(\text{CH}_2)_2\text{SH}$  in  
16  
17 *i*-PrOH solution, saturated with  $\text{N}_2\text{O}$  and irradiated until a total dose of 6 kGy. We used a 10-fold  
18  
19 scale of starting substrates compared to the experiment of the time courses in Fig. 2 (cf.  
20  
21 Supporting Information). Silica gel chromatography on the crude reaction mixture allowed for a  
22  
23 quantitative recovery of the starting fatty acid equivalents. With *n*-hexane the fraction containing  
24  
25 the geometrical isomer mixture of methyl esters was first isolated, corresponding to a 55% yield  
26  
27 (of the ‘thermodynamic’ isomer mix  $L_{EE}:L_{ZE}:L_{EZ}:L_{ZZ} = 70/13/13/4$ ), leaving 45% molar  
28  
29 equivalents to be accounted for.  
30  
31  
32

33  
34 A second fraction eluting with *n*-hexane was isolated, containing a mixture of fatty acid ester  
35  
36 dimers, “L-L”, of general formula **3**, in a 7% yield. The dimeric products can derive from the  
37  
38 bisallylic radical coupling in the conjugated form occurring either in positions 9 and 13. The  
39  
40 dimer formation was already reported in our previous study of methyl linoleate reactivity.<sup>19</sup>  
41  
42  
43

44 **Chart 1.** Lipid dimer products



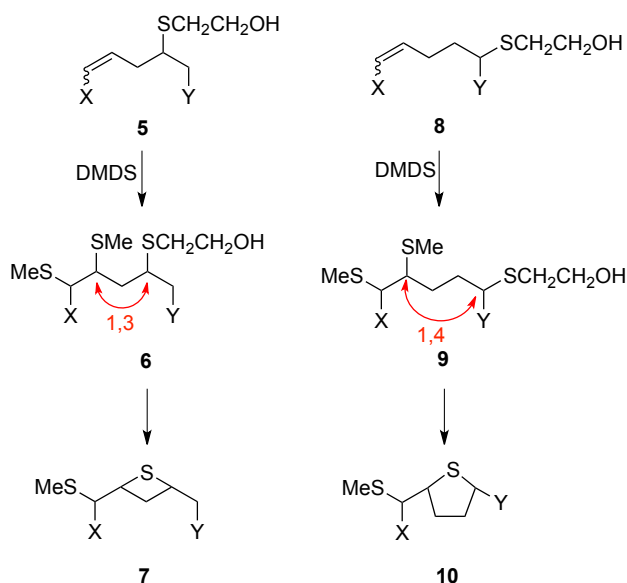
52 Next the mixture of thiol-linoleate addition products eluted (8:2 *n*-hexane/diethyl ether) and  
53  
54 was isolated in 25% yield based on the recovered linoleate isomers (see below). The rest of the  
55  
56 material (13%) was recovered by washing the silica gel with ethanol, affording a final fraction of  
57  
58  
59  
60

1  
2  
3 very polar compounds. To these latter products, based on the NMR and mass analyses a tentative  
4 structure **4**, “L-SL’H”, was formulated as a mixture of positional and geometric isomers.  
5  
6 Formally, **4** could be obtained by HO(CH<sub>2</sub>)<sub>2</sub>SH addition to conjugated dimer **3** and/or be the  
7  
8 product of cross-termination of the allylic radicals examined below (**13** and **16**) with the  
9  
10 bisallylic radical, **2**.  
11  
12  
13  
14

15  
16 Detailed analytical work was then carried out on the nature of the non-dimer thiol-linoleate  
17  
18 addition products in order to gather information on the preferential site of thiyl radical attack.  
19  
20 <sup>13</sup>C NMR is known to be diagnostic for assigning the ethylenic carbon atom resonances of fatty  
21  
22 acid derivatives. In the adduct mixture, eight main signals were present in the range of 126.0-  
23  
24 133.3 ppm, four of which were in an approximately 2:1 ratio with the other four ones, indicating  
25  
26 major and minor addition compounds formed in the reaction. Two signals at 45.1 and 45.8 ppm  
27  
28 can be easily assigned to the C atoms bearing the thiol substituent (see Attached Proton Test  
29  
30 APT experiment in Figure S3 of Supporting Information). On the basis of the C-S resonance 2D  
31  
32 NMR experiments were carried out for the individuation of the main homonuclear and  
33  
34 heteronuclear correlations. In the 2D COSY experiment vinyl H and allylic H were examined, in  
35  
36 particular the 2.23 ppm signal correlated with the multiplets at 2.59 and 2.71 ppm which can give  
37  
38 indication of the allyl proximity to the H alpha to the sulfur substituent in the inside addition  
39  
40 products **15** and **18** resulting as major isomers (see Fig. 5S in Supporting Information). These  
41  
42 two multiplets and the resonance of the C atom bearing the sulfur substituents were then  
43  
44 examined for long distance inverse correlation between carbon and hydrogen atoms using  
45  
46 bidimensional NMR experiments (HMQC, Heteronuclear Multiple-Quantum Correlation and  
47  
48 HMBC, Heteronuclear Multiple Bond Correlation). In the HMQC experiment (see Figure S6) the  
49  
50 correlation between H and C atoms resonances can be obtained. It showed that signals at 45.1  
51  
52  
53  
54  
55  
56  
57  
58  
59  
60

and 45.8 ppm were connected to the multiplets at 2.59 and 2.71 ppm (C and H atoms bonded to the sulphur substituents). In the HMBC experiment the connectivity of the vinyl carbon atoms with the carbon and hydrogen atoms at homoallylic positions (2-atom distance) and with the carbon bearing the thiol moiety could be individuated (Figure S7 in Supporting Information). Indeed, this cross-correlation was individuated for two positional isomers that derive from the internal addition of the thiol moiety to the linoleic double bond (adducts **5** in Scheme 3) as the minor compounds. Two major isomers can have instead one carbon atom resonance with a connectivity between the double bond and the C bearing the sulfur substituent (adduct **8**), whereas the second atom resonance is too remote to give such connectivity. Therefore, the HMBC experiment (see Supporting Information and Figure S7) resulted in the clarification of the adduct mixture, formed by different isomeric structures not only compatible with the straightforward thiol-ene coupling.

### Scheme 3. Constitution of Non-Dimer Products



for compound **5**, **6**, **7**: (a) X=C<sub>5</sub>H<sub>11</sub>, Y=C<sub>9</sub>H<sub>17</sub>O<sub>2</sub>  
 (b) X=C<sub>9</sub>H<sub>17</sub>O<sub>2</sub>, Y=C<sub>5</sub>H<sub>11</sub>  
 for compound **8**, **9**, **10**: (a) X=C<sub>4</sub>H<sub>9</sub>, Y=C<sub>9</sub>H<sub>17</sub>O<sub>2</sub>  
 (b) X=C<sub>8</sub>H<sub>15</sub>O<sub>2</sub>, Y=C<sub>6</sub>H<sub>13</sub>

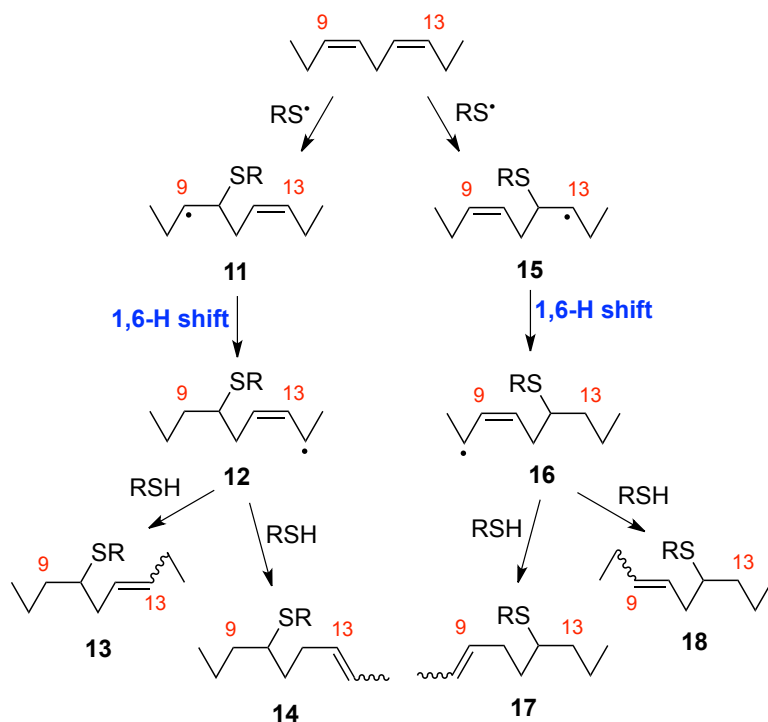
1  
2  
3 Further investigation focused on the assignment of double-bond position of in the thiol-  
4 linoleate adducts. The mixture was treated with dimethyldisulfide (DMDS) under appropriate  
5 conditions to form the corresponding DMDS adducts. This reagent is mostly used in mass  
6 spectrometry of biological lipids, to assign the unsaturation position.<sup>34,35</sup> DMDS compounds give  
7 selective fragmentation by electron impact according to the position the former double bond,  
8 with the EI mass spectrum giving diagnostic fragments to assign the structures. We performed  
9 GC/MS analysis of the reaction monitoring the formation of the DMDS adducts (cf., adducts **6**  
10 and **9**). However, the DMDS adducts were inseparable, giving only one GC peak and molecular  
11 mass of the adducts ( $m/z$  448,  $M^+ - H_2O$ ). The fragmentation masses were complex and did not  
12 allow the product attribution (data not shown).  
13  
14  
15  
16  
17  
18  
19  
20  
21  
22  
23  
24  
25  
26

27 To solve this problem we employed a special method for distinguishing 1,3- from 1,4-  
28 substituted PUFA lipids via rearrangement by elimination of the thiol group and cyclization (per  
29 Scheme 3).<sup>35</sup> Thus, we heated the DMDS adducts mixture at 50 °C in *n*-hexane to form cyclic  
30 sulfides (compounds **7** and **10**, respectively) and were gratified to see four separable compounds  
31 detected by GC/MS analysis, all having  $m/z$  374. The pattern of these four compounds is due to  
32 the DMDS reaction and subsequent rearrangement with formation of two major and two minor  
33 compounds in a 2:1 ratio (product separation and the GC/MS fragmentation patterns are shown  
34 in the SI, Figures S7 and S8). These cyclic-sulfur-rearrangement products (Scheme 3) afford a  
35 suite of ions, derived from the fragmentation of the adjacent positions of the thioether cycle,  
36 which differ as per the location of the ring and the SMe substituent in structures **7** and **10**. This  
37 allowed the position of the SCH<sub>3</sub> moiety to be localized, thus determining the position to the  
38 original double bond in the thiol-ene coupling products. In this way, strong evidence was  
39  
40  
41  
42  
43  
44  
45  
46  
47  
48  
49  
50  
51  
52  
53  
54  
55  
56  
57  
58  
59  
60

obtained that the major adduct isomers contained the double bond shifted to the C8-C9 or C13-C14 positions.

Product analysis thereby established that the adducts were formed via Scheme 4; from which it is evident that the preferred addition-rearrangement of the thiyl radical was at the "inside" carbon atom of the double bonds (**11** and **15**), with subsequent radical translocation by fast 1,6-H shift to form more-stable allyl radicals (**12** and **16**, resp.). From the different distribution of the radical center in the allylic forms, the hydrogen donation of thiol gives un-shifted and shifted addition products **13**, **18** and **14**, **17**, respectively, in a 1:2 ratio. It is worth mentioning that  $^{13}\text{C}$  and  $^1\text{H}$  NMR indicated a trans/cis ratio of approximately 4/1 for each adduct probably due to thiyl radical catalyzed post-isomerization process after their formation.<sup>16</sup>

#### Scheme 4. Inside-addition Pathways



**Laser Flash Photolysis.** It has been previously reported that  $\text{HO}(\text{CH}_2)_2\text{S}^*$  radicals react with linoleic acid with a rate constant of  $3.1 \times 10^7 \text{ M}^{-1}\text{s}^{-1}$  to give the bisallylic radical using pulse radiolysis.<sup>28</sup> In this section we attempt to readdress this reactivity and report detailed kinetic studies of this key reaction step and intermediate using photolytic techniques. Laser flash photolysis (266 nm,  $\sim 10 \text{ ns}$ , up to 10 mJ) of  $\text{O}_2$ -free *t*-BuOH solutions containing  $\text{HO}(\text{CH}_2)_2\text{SH}$  (33 mM) and methyl linoleate (7 mM) gave the spectrum shown in Fig. 3, which is similar to that obtained by pulse radiolysis in  $\text{H}_2\text{O}/\text{EtOH}$  solution and assigned to pentadienyl radical formed by reaction 1.<sup>28</sup>

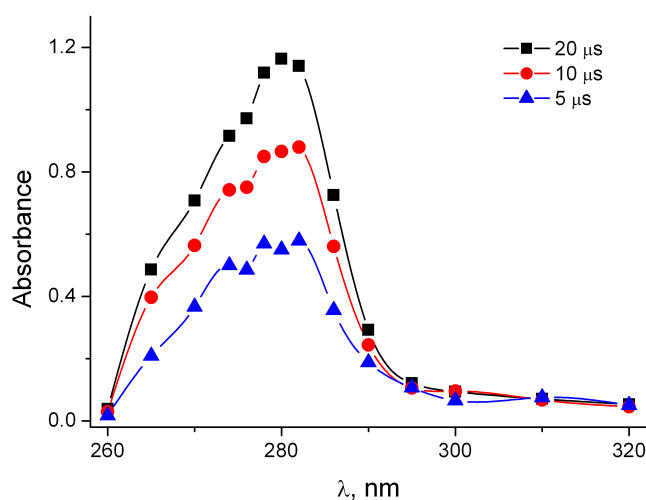


**Figure 3.** Transient absorption spectra obtained at 5, 10 and 20  $\mu\text{s}$  after laser pulse (266 nm) of 33 mM of  $\text{HO}(\text{CH}_2)_2\text{SH}$  and 7 mM of methyl linoleate in argon-saturated *t*-BuOH solution.

It has been reported that  $\text{HO}^*$  radicals react with linoleic acid in aqueous solution producing an intense absorption in the region 282–286 nm with  $\epsilon \sim 30,000 \text{ M}^{-1}\text{cm}^{-1}$ ,<sup>36a</sup> although large quantities of allylic radicals as well as HO-adduct radicals are known to absorb as well in this region.<sup>36b</sup> On the other hand, the reactivity of *t*-BuO $^*$  radical towards methyl linoleate was also measured by indirect methods using laser photolysis techniques.<sup>37</sup> A rate constant of  $8.8 \times 10^6 \text{ M}^{-1} \text{ s}^{-1}$  was

determined with selectivity being ~60% for bis-allylic position and ~40% for the rest of the molecule. There is no doubt that the spectrum in Fig. 3 contains mainly the bis-allylic radical (reaction 1), but it would be also associated to a variety of other minor absorptions from the various transient species and products (see below).

The photochemistry of alkanethiols has been studied in some detail.<sup>38</sup> There is good evidence that reaction 11 is the main path, even though the weakest bond is C-S. Indeed, in gas-phase the photolysis of CH<sub>3</sub>SH at 253.7 nm occurred with  $\Phi \geq 0.9$  and the mechanism consisted with steps 11-13. Similar results were obtained in condensed phase photolysis. For example, photolysis of pure CH<sub>3</sub>CH<sub>2</sub>SH at 253.7 nm afforded hydrogen and ethyl disulfide, the quantum yield values being  $\Phi(\text{H}_2) = \Phi(\text{RSSR}) = 0.25$ .



H<sup>•</sup> atoms are known to react very fast with the bisallylic moiety (eq 14,  $k_{14} = 4.7 \times 10^9 \text{ M}^{-1} \text{ s}^{-1}$ )<sup>32</sup> by H-abstraction from the bisallylic position and addition to the double bond. Moreover, H<sup>•</sup> atoms react with  $\beta$ -mercaptoethanol by two distinct paths. Apart from the expected hydrogen abstraction (Reaction 12,  $k_{12} = 1.7 \times 10^9 \text{ M}^{-1} \text{ s}^{-1}$  for HO(CH<sub>2</sub>)<sub>2</sub>SH), a homolytic substitution at sulfur is also effective as shown in Reaction 15 ( $k_{15} = 3.3 \times 10^8 \text{ M}^{-1} \text{ s}^{-1}$ ), the preference being 5:1 in favor of hydrogen abstraction.<sup>32</sup>



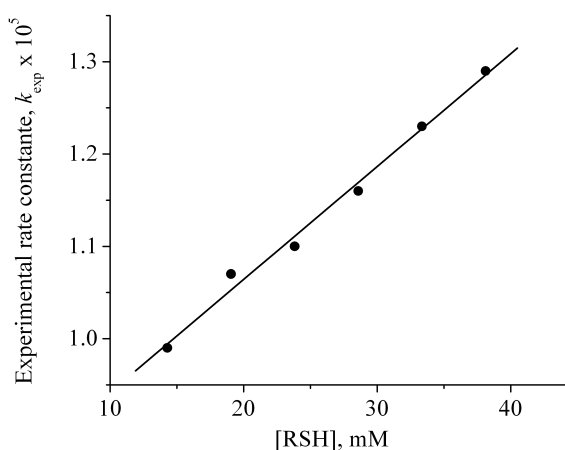


1  
2  
3 From eq 18, a rate constant  $k_{16} = 9.7 \times 10^6 \text{ M}^{-1} \text{ s}^{-1}$  is calculated at 293 K which is 3 times  
4 slower than the value reported for the reaction of  $\text{HOCH}_2\text{CH}_2\text{S}^*$  with linoleic acid by pulse  
5 radiolysis in  $\text{H}_2\text{O}/\text{EtOH}$  solution.<sup>28</sup> The rate constants reported for  $k$  represent the *overall*  
6 reactivity of methyl linoleate towards thiyl radicals (reaction 16). Thus, it is interesting that our  
7 Arrhenius parameters are very similar to those reported for the reactions of *t*-BuO<sup>\*</sup> radical with  
8 cyclopentadiene:  $\log(A/\text{M}^{-1}\text{s}^{-1}) = 8.21$  and  $E_a = 1.85 \text{ kcal/mol}$ , representing the sum of H-  
9 abstraction and addition pathways.<sup>39</sup>

10  
11 Analogous experiments by replacing the methyl linoleate ( $\text{L}_{ZZ}$ ) with the all trans form, methyl  
12 linolelaidate ( $\text{L}_{EE}$ ) have also been carried out and reported in Supporting Information. In  
13 summary, a similar spectrum was observed under identical experimental conditions (Figure (S3))  
14 and a plot of  $k_{\text{exp}}$  vs.  $[\text{L}_{EE}]$ , indicated the slightly lower value of  $8.2 \times 10^6 \text{ M}^{-1} \text{ s}^{-1}$ .<sup>31</sup>

15  
16 In Fig 4 the plots  $k_{\text{exptl}}$  vs.  $[\text{L}_{ZZ}]$  yield quite large intercepts, i.e.,  $k_{01}$  in eq 17 is about  $10^5 \text{ s}^{-1}$ .  
17 This value should include all pseudo-first-order modes of decay of thiyl radical other than its  
18 reaction with methyl linoleate and/or the reverse reaction. In our product studies, we observed  
19 only conjugated *dimers* of pentadienyl radical excluding any formation of conjugated dienes due  
20 to the reversible step. These observations led us to investigate accurately the thiol-dependence of  
21 the transient species absorbing at 280 nm. A series of samples containing methyl linoleate (7  
22 mM) and variable concentrations of  $\text{HO}(\text{CH}_2)_2\text{SH}$  (14-38 mM) were prepared in  $\text{O}_2$ -free *t*-BuOH.  
23 In order to maintain the same concentration of thiyl radical during the experiments, the laser  
24 energy was decreased inversely when the concentration of thiol increases.<sup>31</sup> All measurements  
25 have been made at  $T = 295 \pm 2 \text{ K}$ . In all cases a clean first-order growth due to pentadienyl  
26 radical monitored at 280 nm was detected after the laser pulse. The new experimental pseudo-  
27 first order rate constant rate constant ( $k_{\text{exp}}$ ) is correlated to thiol concentration. Figure 5 shows the  
28  
29  
30  
31  
32  
33  
34  
35  
36  
37  
38  
39  
40  
41  
42  
43  
44  
45  
46  
47  
48  
49  
50  
51  
52  
53  
54  
55  
56  
57  
58  
59  
60

1  
2  
3 linear dependence and from the plot of  $k_{\text{exp}}$  vs.  $[\text{HO}(\text{CH}_2)_2\text{SH}]$  yields a slope of  $(1.2 \pm 0.6) \times 10^6$   
4  
5  $\text{M}^{-1} \text{s}^{-1}$  at 295 K. Thus, the grow-in rate constant of the 280-nm transient absorption is  
6  
7 determined by the total  $\text{S}\bullet$ -reactivity of the solution, of which  $1.2 \times 10^6 \text{M}^{-1} \text{s}^{-1} [\text{SH}]$  comes from  
8  
9 the reagent (presumably via H-abstraction ability), and  $9.7 \times 10^6 \text{M}^{-1} \text{s}^{-1} [\text{L}_{\text{ZZ}}]$  from the lipid  
10  
11 substrate. The *pentadienyl moiety* acts like the probe reagent in a similar way to ketyl radical  
12  
13 derived from diphenylmethanol, acting as probe for competing “invisible” addition or abstraction  
14  
15 reactions of substrates with *t*-BuO $\bullet$  radicals.<sup>40</sup>  
16  
17  
18  
19



37 **Figure 5.** Plot of  $k_{\text{exp}}$  vs.  $\text{HO}(\text{CH}_2)_2\text{SH}$  concentration at 294 K.

38  
39 The thiyl radical-quenching total activity of the lipid is the sum of reactions that are  
40 irreversible in the observed LFP / radiolysis time window ( $10^{-6}$  to  $10^{-5}$  s). Normal double bond  
41 addition is fully and rapidly reversible and energetically unfavorable so it does not quench the  
42 thiyl radical. Whereas, the 1,6-H-atom transfer observed in our product studies (see above) leads  
43 to an allylic radical that would (only slowly) react with SH to regenerate an  $\text{S}\bullet$ . The bisallylic H-  
44 abstraction itself must be much slower otherwise the reaction product yield would be dominated  
45 by conjugated products (i.e., the lipid dimer **3**, L-L). The early-period yield of dimer (4%)  
46 indicates that the abstraction reaction is ~15-fold slower than  $\text{S}\bullet$  addition/isomerization. We  
47  
48  
49  
50  
51  
52  
53  
54  
55  
56  
57  
58  
59  
60

1  
2  
3 therefore ascribe the fast quenching reaction to the rapid collapse of the *inside*-addition adduct  
4  
5 ( $SL_i^\bullet$ ) to afford slow reacting allyl radical ( $SL'^\bullet$ ). The yield of the reduced rearranged adduct  
6  
7  $SL'^\bullet$ ,  $SL'H$ , indicates that (i) it is the inside addition that affords the pathway to H-abstraction,  
8  
9 and (ii) it is the pathway that produces the observed thiyl radical quenching that is observed for  
10  
11 the 280 nm chromophore. To elaborate on the evident mechanism, we turned to quantum  
12  
13 mechanical investigations of the elementary steps.  
14  
15  
16  
17

18 **DFT Calculations** at the B3LYP/6-31+G\*\* level were performed to determine the activation  
19  
20 enthalpy  $\Delta H_Z^\ddagger$  and free energy  $\Delta G_Z^\ddagger$  as well as the rate constants  $k_Z$  at 20 °C for the addition of  
21  
22 the thiyl radical  $HO(CH_2)_2S^\bullet$  to the C–C double bonds of (3*Z*,6*Z*)-nona-3,6-diene (**19**), as a model  
23  
24 for linoleic acid methyl ester ( $L_{ZZ}$ ).  
25  
26  
27

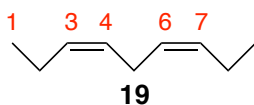
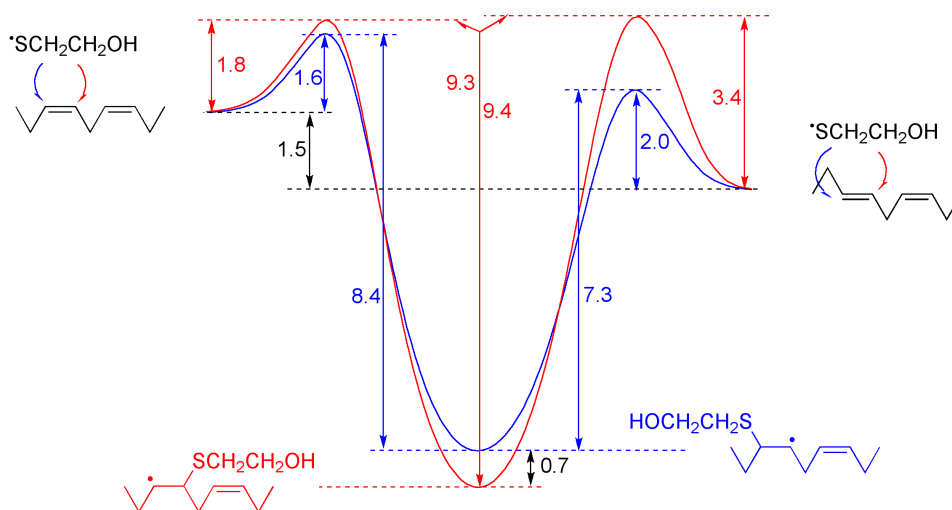


Figure 6 shows that the enthalpy barriers for the addition of the thiyl radical to the C–C double bond is computed to be small, being  $\Delta H_Z^\ddagger$  equal to 1.6 and 1.8 kcal/mol for addition to C3 (blue) and C4 (red), respectively. The  $\Delta G_Z^\ddagger$  (C3) = 13.1 and  $\Delta G_Z^\ddagger$  (C4) = 13.5 kcal/mol were also calculated. From the transition-state theory the theoretical rate constants are computed to be  $k_Z(C3) = 2.4 \times 10^4$  and  $k_Z(C4) = 1.2 \times 10^4 \text{ M}^{-1} \text{ s}^{-1}$  using the activation free energy computed by estimating the entropy contributions from frequency calculations. These values are similar to those computed previously for addition of  $HO(CH_2)_2S^\bullet$  to *Z*- and *E*-isomers of 2-butene.<sup>18,41</sup> The radical addition is exothermic, the reaction enthalpy  $\Delta H_Z$  being 6.8 and 7.5 kcal/mol for thiyl addition to C3 and C4, respectively. That is, the C4-thiyl adduct (red) is more stable than the C3-thiyl adduct (blue) by 0.7 kcal/mol. The enthalpy barrier for the reverse reaction ( $\beta$ -fragmentation) is computed to be larger, being  $\Delta H_{-Z}^\ddagger(C3) = 8.4$  and  $\Delta H_{-Z}^\ddagger(C4) = 9.3$  kcal/mol.

From the free energy barriers  $\Delta G_{-Z}^{\ddagger}(\text{C3}) = 6.9$  and  $\Delta G_{-Z}^{\ddagger}(\text{C4}) = 8.4$  kcal/mol, the rate constants for  $\beta$ -fragmentation  $k_{-Z}(\text{C3}) = 4.7 \times 10^7 \text{ s}^{-1}$  and  $k_{-Z}(\text{C4}) = 3.3 \times 10^6 \text{ s}^{-1}$  are calculated. The same trend was previously found for the thiyl addition to *Z*-2-butene.<sup>42</sup>



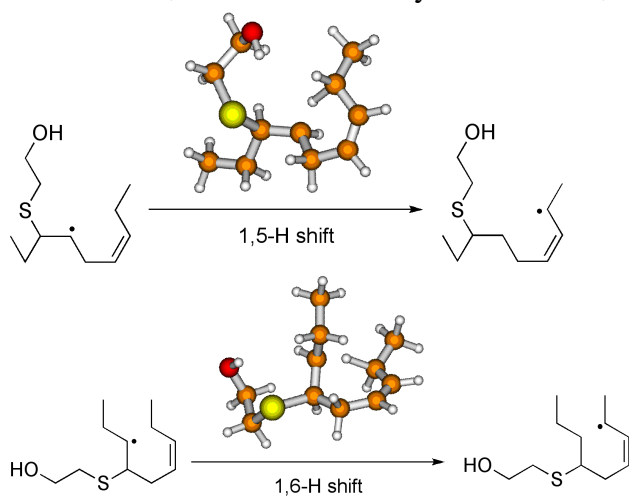
**Figure 6.** Modeling  $L_{ZZ} \rightleftharpoons L_{EZ}$ , the enthalpy profile in kcal/mol for the isomerization of (3*Z*,6*Z*)-nona-3,6-diene (**19**) to (3*E*,6*Z*)-nona-3,6-diene by  $\text{HOCH}_2\text{CH}_2\text{S}^*$  radical; blue is the outside and red and the inside attack of thiyl radical.

It should be noted that the computed rate constants for addition of  $\text{HO}(\text{CH}_2)_2\text{S}^*$  to C3 and C4 positions – the outside (blue) and inside (red) positions – are comparable, while the rate constant for the reverse  $\beta$ -fragmentation at C3 is an order of magnitude faster than at C4. On the other hand, the rate constant for  $\beta$ -fragmentation of the C3-thiyl adduct leading to the *E,Z* isomer is faster ( $k_E(\text{C3}) = 8.4 \times 10^7 \text{ s}^{-1}$ ), whereas that of the C4-thiyl adduct is slower ( $k_E(\text{C4}) = 1.6 \times 10^5 \text{ s}^{-1}$ ) than the corresponding  $\beta$ -fragmentation reaction leading to the *Z,Z* isomer. Thus, the concentration of the (inside) C4-adduct in solution should be much higher than that of the (outside) C3-adduct. This can explain why product analysis indicates that the radical adduct undergoes 1,6-hydrogen atom translocation (cf. Scheme 4). In Supporting Information, Table S5

summarizes  $\Delta H^\ddagger$ ,  $\Delta G^\ddagger$ , and  $k$  for all additions and fragmentation steps, together with Figure S4 and S5 that shown enthalpy barriers of H-atom abstraction vs. additions and enthalpy profile for the isomerization of pentadienyl radical.

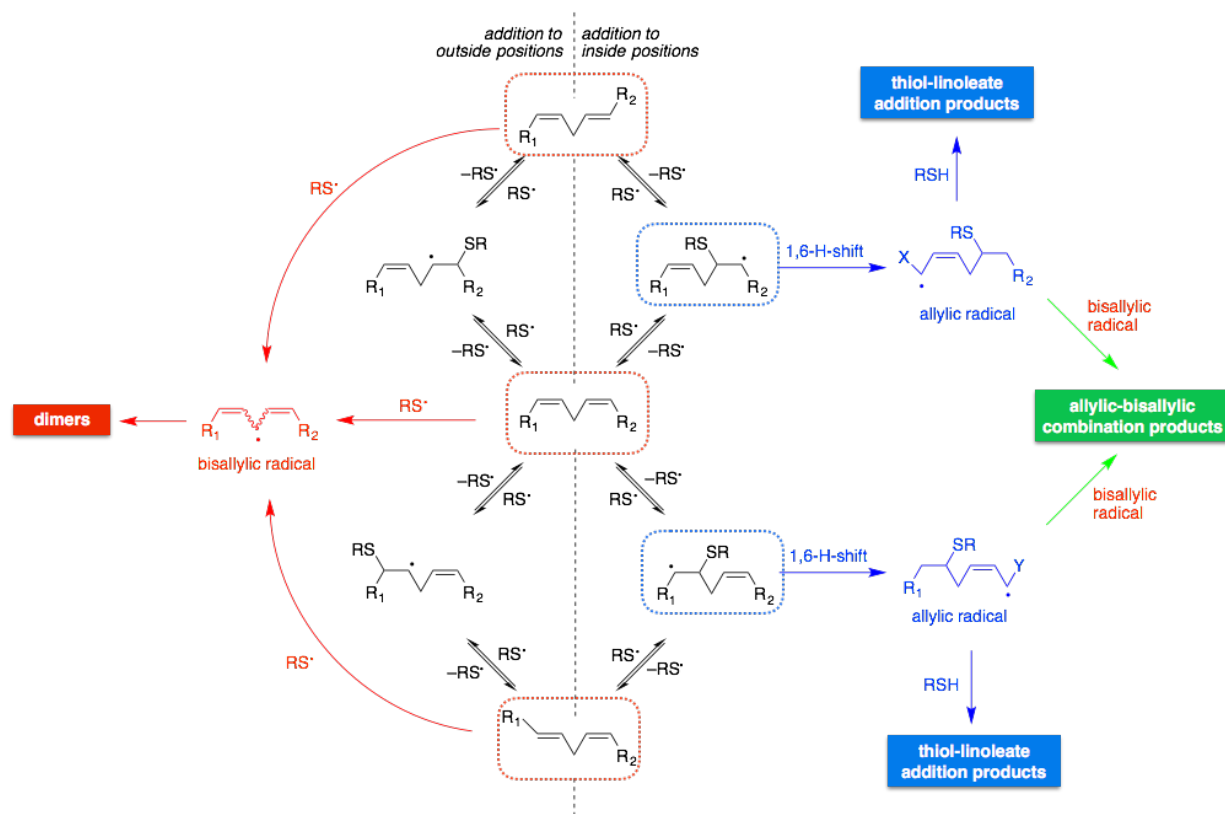
We also investigated theoretically the radical translocation that is defined in product studies, although the transition state of a simple model like **19** is expected to be quite different from methyl linoleate both in terms of entropy and enthalpy. Both 1,5 H-shift of C3-thiyl adduct and 1,6 H-shift of C4-thiyl adduct are considered for comparison (Scheme 5). DFT calculation at the B3LYP/6-31+G\*\* level shows that that the enthalpy barrier for the 1,5 H-shift in the C3-adduct ( $\Delta H_Z^{1,5H^\ddagger} = 15.8$  kcal/mol) is slightly higher than for the 1,6 H-shift in the C4-adduct ( $\Delta H_Z^{1,6H^\ddagger} = 15.5$  kcal/mol). As expected, both reactions are computed to be strongly exothermic, the reaction enthalpy being -14.7 and -14.2 kcal/mol for the 1,5 H-shift and 1,6 H-shift. It is worth mentioning the kinetic work of 1,5 H-transfer from mono-, di- and tri-aryl substituted positions or 1,6 H-transfer reactions from di- and tri-aryl substituted measured by laser flash photolysis.<sup>43</sup> For a matched pair of 1,5 and 1,6 H-transfers, the enthalpy of activation favors the 1,6 H-transfer.

**Scheme 5.** 1,5 H-shift of C3-thiyl adduct vs. 1,6 H-shift of C4-thiyl adduct



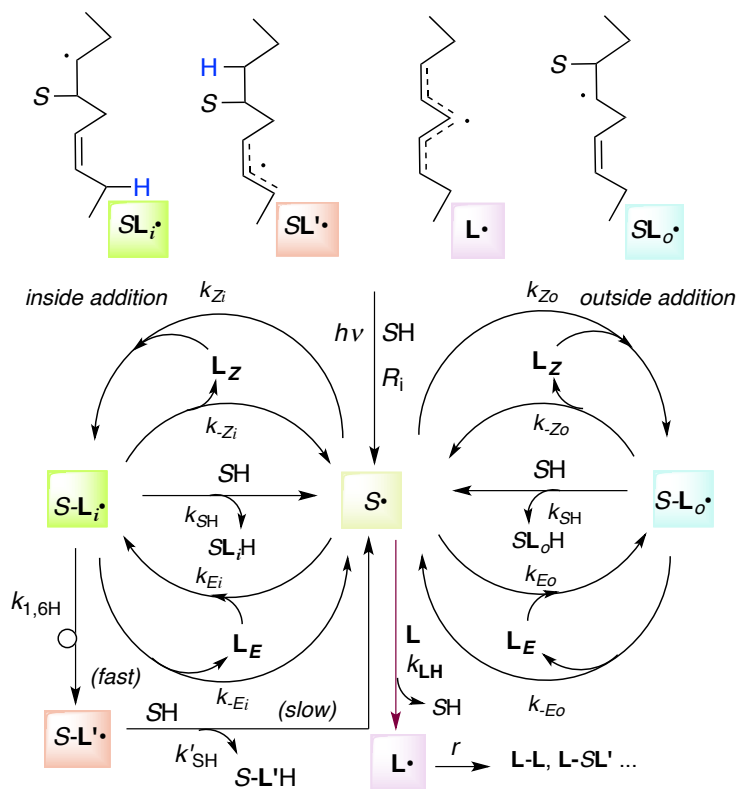
1  
2  
3  
4       **Overall Mechanism Proposal.** Our product studies approach allowed us to propose the  
5  
6 mechanism of methyl linoleate transformation by  $\text{HO}(\text{CH}_2)_2\text{S}^{\bullet}$  radical. In Scheme 6 are indicated  
7  
8 the thiol-addition products with unshifted and shifted double bond (in blue) together with the  
9  
10 formation of conjugated dienes (in red) and allylic-bisallylic combination products (in green).  
11  
12 Scheme 6 shows also that  $\text{HO}(\text{CH}_2)_2\text{S}^{\bullet}$  either abstracts hydrogen from the bisallylic position (red  
13  
14 arrow) or adds reversibly to all possible positions of double bonds (black arrows). The dashed  
15  
16 line separates the site of addition being *outside* (far away from the bisallylic position) or *inside*  
17  
18 (next to the bisallylic position) in analogy with the above described DFT calculations. The rate  
19  
20 constant of  $9.7 \times 10^6 \text{ M}^{-1} \text{ s}^{-1}$  at 20 °C obtained by time-resolved spectroscopy indicates the  
21  
22 overall reactivity of thiyl radical towards methyl linoleate. Our calculations indicate that the rate  
23  
24 constants for the *outside* positions are twice the rate constants for the *inside* positions. If the rate  
25  
26 constants for addition of  $\text{HO}(\text{CH}_2)_2\text{S}^{\bullet}$  to the *outside* and *inside* positions are close to  $3 \times 10^6$  and  
27  
28  $1.5 \times 10^6 \text{ M}^{-1} \text{ s}^{-1}$ , respectively,<sup>21</sup> and taken the statistical factors of two double bonds, the H-  
29  
30 abstraction from the bisallylic position will be close to  $0.7 \times 10^6 \text{ M}^{-1} \text{ s}^{-1}$ . On the other hand, our  
31  
32 calculations show that due to the combination of the rate constants effects for the various reverse  
33  
34  $\beta$ -fragmentation steps, the lifetime of the inside-adduct in solution should be much higher than  
35  
36 that of the outside-adduct and long enough to undergo a 1,6-hydrogen atom translocation with a  
37  
38 rate constant of  $\sim 10^5 \text{ s}^{-1}$  (blue arrows). The resulting allylic radicals can be quenched by the thiol  
39  
40 affording the four thiol-addition products with unshifted and shifted double bond (in blue). These  
41  
42 reactions cannot be very fast, being thermoneutral or slightly endothermic, and compete with  
43  
44 trapping by bisallylic radical.  
45  
46  
47  
48  
49  
50  
51  
52  
53  
54  
55  
56  
57  
58  
59  
60

Scheme 6. Overall mechanism proposal



**Steady-state Radical-Chain Kinetics.** Given the foregoing mechanism and the estimated key rate constants, we can express the kinetics for the catalytic cycle as a radical chain propagating the cis to trans interconversion. The degraded-chain for the PUFA (Scheme 7) is more complicated than for MUFAs or simple alkenes (cf.<sup>21</sup>): the DBs are non-symmetrical and side reactions divert the chain. In either system, however, the overall reaction rate will be proportional to the thiyl radical concentration,  $[S\bullet]$ . Scheme 7 is set up for steady-state radical-concentration analysis. The right-hand “bulb” represents isomerization and thiol-ene coupling (TEC) resulting from outside addition to the bisallylic group. The bulb on the left for inside addition is the same except that it *leaks* radical centers into allylic radicals  $SL\bullet$  via 1,6-H transfer in the inside adduct  $SL\bullet$ . At all but very high  $[SH]$ , the conventional TEC reaction (center of bulb) will have negligible impact on yields and rates.

## Scheme 7. Kinetic Model for PUFA-thiol Reaction



Assuming uniform radical-radical termination,<sup>17,21</sup> the total radical concentration obeys the stasis equation “radical initiation = radical-radical termination”,  $R_i = 2k_t[\cdot]^2$  or

$$[\cdot] = (R_i/2k_t)^{1/2} = R_i/r \quad (19)$$

$$[\cdot] = [S\cdot] + [SL_i\cdot] + [SL_o\cdot] + [SL'\cdot] + [L_{-H}\cdot] \quad (20)$$

$$[\cdot]/[S\cdot] = 1 + SL_i\cdot/S\cdot + SL_o\cdot/S\cdot + SL'\cdot/S\cdot + L_{-H}\cdot/S\cdot \quad (21)$$

where  $r = (R_i/2k_t)^{1/2}$  the first-order termination rate constant for any radical in the initiated system.<sup>21</sup>

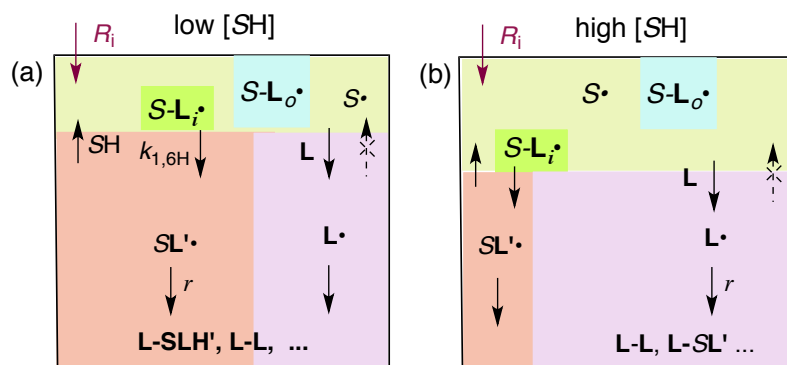


**Figure 7.** Radical center distributions for hydrothiolation of a PUFA lipid, per Scheme 7, at (a) low and (b) high thiol concentrations.

This pool of radical centers is split between the reacting species (eq 20). The molar ratios of these species (eq 21) are determined by the flows of radical centers between species – i.e., by the steady-state equations (as sketched in Fig. 7, e.g.)

As the rates of isomerization and coupling are both proportional to  $[S\bullet]$ , the ratio  $[\bullet]/[S\bullet]$  (eq 21) signifies the general retardation caused by the formation of other radicals from  $S\bullet$ .

For example, a steady-state for the bisallylic radical  $L_{-H}\bullet$ , requires

rate of gain = rate of loss

$$[S\bullet]k_{LH}[L] = [L_{-H}\bullet] \times r$$

$$L_{-H}\bullet/S\bullet = k_{LH}[L]/r \quad (22)$$

With typical values  $k_{LH}[L] \sim 10^3 \text{ s}^{-1}$  and  $r \sim 50 \text{ s}$ , eq 22 indicates a steady-state ratio  $L_{-H}\bullet/S\bullet > \sim 20$ , meaning that the thiyl  $S\bullet$  will be less than 5% of the total radical population in Fig. 7. Regardless of other equilibria, this *self-inhibition* reaction will strongly retard the chain. The formation of the mono-allylic radical  $SL'\bullet$  via 1,6-H transfer will further retard the chain. The total rate retardation factor is found by summing over species and simplifying.<sup>31</sup> The resulting

kinetic equation can conveniently be expressed in terms of the length,  $\delta = -d[\mathbf{L}_{ZZ}]/dt/R_i$ , of the free radical chain or cycle

$$1/\delta \approx 1/\delta_{\text{LH}} + 1/\delta_{1,6\text{H}} \quad (23).$$

Where the bisallylic H-abstraction-*inhibited* chain length

$$\delta_{\text{LH}} = 2k_{\text{iso}}/k_{\text{LH}} \quad (24);$$

i.e., it is fixed to the rate ratio of isomerization to H-abstraction. While the 1,6-H transfer *retarded* chain length results from the balance between formation, reaction and termination of allylic  $\text{SL}'\bullet$

$$\delta_{1,6\text{H}} = (k_{\text{iso}}/k_{\text{zi}})(1 + k_{\beta\text{i}}/k_{1,6\text{H}})(1 + k'_{\text{H}}[\text{SH}]/r) \quad (25).$$

The shorter of these chains will determine the overall kinetic chain length,  $\delta$ , and isomerization rate,  $v_{\text{iso}} = R_i \delta = -d[\mathbf{L}_{ZZ}]/dt$ .

Our data suggest that at higher [SH], the  $\mathbf{L}_{\text{H}}\bullet$  radical dominates the steady state, as evidenced by the dominance of lipid dimer  $(\mathbf{L}_{\text{H}})_2$  among the termination products. Whereas at low thiol concentrations the allylic radical  $\text{SL}'\bullet$  may build up and react instead with the  $\mathbf{L}_{\text{H}}\bullet$  radical to give the cross-termination product  $\mathbf{L}_{\text{H}}\text{-SL}'\text{H}$  (i.e., **4**), as indicated in Fig. 7a and as indeed was found under dilute conditions.

Conjugated groups are strong inhibitors of double-bond isomerization.<sup>42,43</sup> However, upon its build-in, the conjugated lipid dimer  $(\mathbf{L}_{\text{H}})_2$  (**3**) will undergo addition of  $S\bullet$  radicals to form allylic adducts,  $S\bullet + (\mathbf{L}_{\text{H}})_2 \rightarrow S\text{-}(\mathbf{L}_{\text{H}})_2\bullet + \text{SH} \rightarrow S\text{-L}'\text{H-L}$ . At higher thiol concentrations, these may contribute to the yield of cross-termination product **4** ( $\mathbf{L}\text{SL}'\text{H}$ ).

1  
2  
3 Biological lipids contain mixtures of PUFAs and MUFAs. Per the self-inhibition model, the  
4 rate of isomerization of the double bonds in the MUFA component of such mixtures is expected  
5 to be retarded to the same extent as for the double bonds in the PUFA component. Which again  
6 is as observed<sup>1,16,19</sup> and which demonstrates the retarding effect of the build-up of non-  
7 propagating radicals like  $\mathbf{L}_{\text{H}}\bullet$  (cf. Fig. 7 and eqs 21–23).  
8  
9

10  
11  
12  
13  
14  
15  
16 Although the present work is dealing without molecular oxygen, a final consideration on the  
17 previous observations is needed in view of our new results and since living systems typically  
18 contain  $\text{O}_2$ , and  $\text{O}_2$  rapidly traps carbon radicals. In the light of self-inhibition, the intriguingly  
19 small effect of  $\text{O}_2$  on the thiol reaction rate of PUFAs at physiologically relevant levels ( $[\text{O}_2] \leq$   
20  $0.24 \text{ mM}$ ) reflects that without  $\text{O}_2$  most radicals in the anoxic system are *already* non-  
21 propagating ( $\mathbf{L}_{\text{H}}\bullet$ ) or slow-propagating ( $\mathbf{SL}\bullet$ ) species, and that the propagating carbon radicals  
22 ( $\mathbf{SL}\bullet$ ) are too short-lived to be effectively trapped by the  $\text{O}_2$ . Quantitatively: (i) fragmentation of  
23  $\mathbf{SL}\bullet$  is  $\sim 100$ -fold *faster* than oxygen trapping<sup>19</sup>  $k_{\beta}$  ( $\sim 10^8 \text{ s}^{-1}$ )  $\gg k_{\text{O}_2}[\text{O}_2]$  ( $\sim 10^6 \text{ s}^{-1}$ ). The  $\text{O}_2$  will  
24 therefore only hinder cycles longer than  $\delta \sim 100$ , meaning that it will hamper MUFA (400) but  
25 not PUFA isomerization ( $\delta \approx 14$ ) (as observed); (ii) peroxy radicals react slowly with an alkyl  
26 thiol in a thermoneutral reaction ( $D_{\text{RS-H}} \approx D_{\text{LOO-H}} \approx 87 \text{ kcal/mol}$ ) that restarts the chain.<sup>46</sup> Finally,  
27 (iii) the known addition of oxygen to the thiol is fast but reversible ( $\text{RS}\bullet + \text{O}_2 \rightleftharpoons \text{RSOO}\bullet$ ,  
28  $K_{\text{S},+\text{O}_2}[\text{O}_2] = 3,000 \text{ M}^{-1}[\text{O}_2] \approx 0.7$ )<sup>47</sup> and so – inhibition being additive – will have no effect on the  
29 auto-inhibited chain. Accordingly, the isomerization rate in methyl linoleate and 85 mM RSH in  
30 *t*-BuOH solution was 45% faster with 0.24 mM  $\text{O}_2$  than without, but at lower [thiol] the  $\text{O}_2$  had  
31 negligible effect. Oxygen likewise has negligible effect on the rate of thiol-catalyzed cis-to-trans  
32 isomerization in biomimetic systems, even though substantial lipid hydroperoxides ( $\mathbf{L}_{\text{H}}\text{OOHs}$ )  
33 may form during reaction.<sup>22a</sup>  
34  
35  
36  
37  
38  
39  
40  
41  
42  
43  
44  
45  
46  
47  
48  
49  
50  
51  
52  
53  
54  
55  
56  
57  
58  
59  
60

1  
2  
3 All-in-all, isomerization kinetics of PUFA-lipid double-bonds in solution can be solved using  
4 conventional steady-state methods, but which must then include the unheralded retarding effect  
5 of minor side-chains including both *inter*- and *intra*-molecular lipid H-abstraction. Notably, the  
6 observed rates and trends in solution phase can now be quantitatively explained without resort to  
7 ad hoc mechanisms for the dramatic decline in isomerization rate with the lipid's PUFA content.  
8  
9

## 15 Conclusions

17  
18 A multi-pronged approach has been used to solve one of the most intriguing free radical  
19 reactions among biomolecule transformations, i.e., the reaction of the PUFA model, methyl  
20 linoleate, with sulfur-centered radicals. A detailed reaction mechanism has been determined by  
21 combining data from parallel methods of radical generation (photolysis and radiolysis), detailed  
22 analysis of product constitutions, matched time-resolved spectroscopy measurements (laser flash  
23 photolysis), in tandem with DFT calculations and steady-state radical-chain kinetics.  
24  
25  
26  
27  
28  
29  
30  
31

32 Thiyl radical addition to the double bond is estimated to be little bit faster than H-abstraction  
33 from the bisallylic position, affording a catalytic cycle length of ~13 *cis-trans* conversions per  
34 initiating radical. During *cis-trans* isomerization under *dilute* conditions, addition to the *inside*  
35 position (i.e., closer to the bisallylic group) leads to a rapid radical translocation via 1,6-  
36 hydrogen transfer, resulting in allylic stabilized intermediates that are reduced by the thiol to four  
37 specific products (cf. Scheme 6).  
38  
39  
40  
41  
42  
43  
44  
45

46 This model study provides valuable new insights into the reactivity of PUFAs and their structural  
47 transformations, which is a lively interdisciplinary field of research with applications of the thiol-  
48 ene reactivity spanning from metabolomics to renewable materials. Indeed, further developments  
49 in these areas can be foreseen, such as cross-linked products formed in mitochondrial PUFA- and  
50 thiol-rich membranes, as well as green products from PUFA-containing oils.  
51  
52  
53  
54  
55  
56  
57  
58  
59  
60

## Acknowledgments

The sponsorship concerned by COST Action CM1201 on “Biomimetic Radical Chemistry” is kindly acknowledged.

## Supporting Information Available

The Supporting Information is available free of charge on the ACS Publications website: (1) materials and methods (2) isomerization experimental conditions with the effect of methyl linoleate and thiol concentrations (3) isomerization of methyl linoleate (4) experiments for the exclusion of conjugated diene formation (5) product isolation and identification with analytical and spectral characterization (6) formation of DMDS adducts and rearrangement to cyclic sulphides (7) Laser flash photolysis details (8) degraded chain kinetic model (9) DFT calculations (10) Absolute energies and coordinates for minimized structures .

## AUTHOR INFORMATION

### Corresponding Author

[chrys@isof.cnr.it](mailto:chrys@isof.cnr.it)

### Present Addresses

<sup>†</sup> ISOF, Consiglio Nazionale delle Ricerche, Via P. Gobetti 101, 40129 Bologna, Italy.

E-mail: [chrys@isof.cnr.it](mailto:chrys@isof.cnr.it); [carla.ferreri@isof.cnr.it](mailto:carla.ferreri@isof.cnr.it)

<sup>§</sup> Retired. Present Email: [guerra.maurizio@alice.it](mailto:guerra.maurizio@alice.it)

<sup>#</sup> Department of Chemistry, United Arab Emirates University, P.O. Box 15551, Al Ain, Abu Dhabi, United Arab Emirates. E-mail: [samadi@uaeu.ac.ae](mailto:samadi@uaeu.ac.ae)

<sup>‡</sup> James Cook University, Cairns 4878 QLD, Australia. Email: [vincent.bowry@jcu.edu.au](mailto:vincent.bowry@jcu.edu.au)

## REFERENCES

- (1) (a) Chatgililoglu, C; Ferreri, C. *Acc. Chem. Res.* **2005**, *38*, 441; (b) Ferreri, C; Chatgililoglu, C. *ChemBioChem* **2005**, *6*, 1722. (c) Ferreri, C; Chatgililoglu, C. In *Encyclopedia of Radicals in Chemistry, Biology and Materials*; Chatgililoglu, C.; Studer, A., Eds; Wiley: Chichester (U.K.), 2012; vol. 3; pp. 1599–1622.
- (2) (a) Chatgililoglu, C.; Ferreri, C.; Melchiorre, M.; Sansone, A.; Torreggiani, A. *Chem. Rev.* **2014**, *114*, 255. (b) See also: Dénès, F.; Pichowicz., M.; Povie, G.; Renaud, P. *Chem. Rev.* **2014**, *114*, 2587. (c) Hung, W-L.; Hwang, L. S.; Shahidi, F.; Pan, M-H.; Wang, Y.; Ho, C-T. *J. Functional Foods* **2016**, *25*, 14.
- (3) (a) Ferreri, C; Kratzsch, S.; Brede, O.; Marciniak, B.; Chatgililoglu, C. *Free Radic. Biol. Med.* **2005**, *38*, 1180; (b) Cort, A.; Ozben, T.; Sansone, A.; Barata-Vallejo, S.; Chatgililoglu, C.; Ferreri, C. *Org. Biomol. Chem.* **2015**, *13*, 1100; (c) Cort, A.; Melchiorre, M.; Chatgililoglu, C.; Ferreri, C.; Sansone, A.; Ozben, T. *Biochim. Biophys. Acta* **2016**, *1858*, 434.
- (4) (a) Zambonin, L.; Ferreri, C; Cabrini, L.; Prata, C; Chatgililoglu, C; Landi, L. *Free Radical Biol. Med.* **2006**, *40*, 1549; (b) Zambonin, L.; Prata, C.; Cabrini, L.; Maraldi, T.; Fiorentini, D.; Vieceli Dalla Sega, F.; Hakim, G.; Landi, L. *Free Radical Biol. Med.* **2008**, *44*, 594; (c) Marini, M.; Abruzzo, P. M.; Bolotta, A.; Veicsteinas, A.; Ferreri, C. *Lipids in Health and Diseases* **2011**, *10*, 188.
- (5) (a) Ferreri, C.; Chatgililoglu, C. *Expert Rev. Mol. Diagn.* **2012**, *12*, 767. (b) Ferreri, C; Chatgililoglu, C. *Membrane Lipidomics for Personalized Health*; Wiley: Chichester (U.K.), 2015.

- 1  
2  
3 (6) (a) Ferreri, C; Angelini, F.; Chatgililoglu, C; Dellonte, S.; Moschese, V.; Rossi, P.; Chini, L.  
4  
5 *Lipids* **2005**, *40*, 661; (b) Puca, A. A.; Andrew, P.; Novelli, V.; Viviani, C; Somalvico, F.;  
6  
7 Cirillo, N. A.; Chatgililoglu, C; Ferreri, C. *Rejuv. Res.* **2008**, *11*, 63. (c) Sansone, A.;  
8  
9 Melchiorre, M.; Chatgililoglu, C.; Ferreri, C. *Chem. Res. Toxicol.* **2013**, *26*, 1703; (d) Sansone,  
10  
11 A.; Tolika, E.; Louka, M.; Sunda, V.; Deplano, S.; Melchiorre, M.; Anagnostopoulos, D.;  
12  
13 Chatgililoglu, C.; Formisano, C.; Di Micco, R.; Faraone Mennella, R.; Ferreri, C. *PLoS ONE*  
14  
15 **2016**, *11*, art. no. e0152378.  
16  
17  
18  
19 (7) (a) Ferreri, C; Samadi, A.; Sassatelli, F.; Landi, L.; Chatgililoglu, C. *J. Am. Chem. Soc.*  
20  
21 **2004**, *126*, 1063; (b) Ferreri, C; Faraone Mennella, M. R.; Formisano, C; Landi, L.;  
22  
23 Chatgililoglu, C. *Free Radic. Biol. Med.* **2002**, *33*, 1516; (c) Melchiorre, M.; Torreggiani, A.;  
24  
25 Chatgililoglu, C.; Ferreri, C. *J. Am. Chem. Soc.* **2011**, *133*, 15184.  
26  
27  
28 (8) Chatgililoglu, C.; Ferreri, C.; Torreggiani, A.; Renzone, G.; Salzano, A.M.; Scaloni, A. *J.*  
29  
30 *Proteomics* **2011**, *74*, 2263.  
31  
32  
33 (9) Chatgililoglu, C.; Ferreri, C.; Masi, A.; Melchiorre, M.; Sansone, A.; Terzidis, M.A.;  
34  
35 Torreggiani, A. *Chimia* **2012**, *66*, 368.  
36  
37  
38 (10) Mozziconacci, O.; Bobrowski, K.; Ferreri, C.; Chatgililoglu, C. *Chem. Eur. J.* **2007**, *13*,  
39  
40 2029.  
41  
42  
43 (11) Kadlcik, V.; Sicard-Roselli, C.; Houée-Levin, C.; Kodicek, M.; Ferreri, C.; Chatgililoglu,  
44  
45 C. *Angew. Chem. Int. Ed.* **2006**, *45*, 2595.  
46  
47  
48 (12) Ferreri, C.; Manco, I.; Faraone-Mennella, M.R.; Torreggiani, A.; Tamba, M.; Manara, S.;  
49  
50 Chatgililoglu, C. *ChemBioChem* **2006**, *7*, 1738.  
51  
52  
53 (13) Ferreri, C.; Chatgililoglu, C.; Torreggiani, A.; Salzano, A.M.; Renzone, G.; Scaloni, A. *J.*  
54  
55 *Proteome Res.* **2008**, *7*, 2007.  
56  
57  
58  
59  
60

- 1  
2  
3 (14) Salzano, A.M.; Renzone, G.; Scaloni, A.; Torreggiani, A.; Ferreri, C.; Chatgililoglu, C.  
4  
5 *Mol. BioSyst.* **2011**, *7*, 889.  
6  
7  
8 (15) Torreggiani, A.; Domènech, J.; Ferreri, C.; Orihuela, R.; Atrian, S.; Capdevila, M.;  
9  
10 Chatgililoglu, C. *Chem. Eur. J.* **2009**, *15*, 6015.  
11  
12 (16) Chatgililoglu, C.; Ferreri, C.; Ballestri, M.; Mulazzani, Q. G.; Landi, L. *J. Am. Chem. Soc.*  
13  
14 **2000**, *722*, 4593.  
15  
16  
17 (17) Chatgililoglu, C.; Altieri, A.; Fischer, H. *J. Am. Chem. Soc.* **2002**, *124*, 12816.  
18  
19 (18) Chatgililoglu, C.; Samadi, A.; Guerra, M.; Fischer, H. *ChemPhysChem* **2005**, *6*, 286.  
20  
21 (19) Ferreri, C.; Costantino, C.; Perrotta, L.; Landi, L.; Mulazzani, Q. G.; Chatgililoglu, C. *J.*  
22  
23 *Am. Chem. Soc.* **2001**, *123*, 4459.  
24  
25  
26 (20) In particular, the process produced neither discernible double-bond migration nor lipid-  
27  
28 termination products, and had an initial rate that was independent from the thiol concentration.  
29  
30  
31 (21) (a) Chatgililoglu, C.; Bowry, V. W. *J. Am. Chem. Soc.*, submitted. (b) As discussed in this  
32  
33 paper, it turns out MUFA isomerization cycles are also non-ideal, though less obviously than  
34  
35 with the PUFAs. Even so, *chain-degradation* from (mono)allylic H-abstraction retards the  
36  
37 MUFA isomerization, resulting in *actual* addition rates constants being ~30-fold faster than  
38  
39 reported effective ones. Fragmentation rates are unaffected.  
40  
41  
42 (22) (a) Mihaljević, B.; Tartaro, I.; Ferreri, C.; Chatgililoglu, C. *Org. Biomol. Chem.* **2011**, *9*,  
43  
44 3541. (b) Tartaro-Bujak, I.; Chatgililoglu, C.; Ferreri, C.; Valgimigli, L.; Amorati, R.;  
45  
46 Mihaljević, B. *Radiat. Phys. Chem.* **2016**, *124*, 104. (c) Tartaro-Bujak, I.; Mihaljević, B.; Ferreri,  
47  
48 C.; Chatgililoglu, C. *Free Radic. Res.* **2016**, *50*, S18.  
49  
50  
51 (23) Frank, H.; Thiel, D.; Macleod J. *Biochem. J.* **1989**, *260*, 873.  
52  
53  
54  
55  
56  
57  
58  
59  
60

- 1  
2  
3 (24) (a) Bantchev, G. B.; Kenar, J. A.; Biresaw, G.; Han, M. G. *J. Agr. Food Chem.* **2009**, *57*,  
4 1282. (b) Desroches, M.; Caillol, S.; Lapinte, V.; Auvergne, R.; Boutevin, B. *Macromolecules*  
5  
6 **2011**, *44*, 2489. (c) Hayashi, T.; Kazlauciusas, A.; Thornton, P. D. *Dyes and Pigments* 2015,  
7 123, 304.  
8  
9  
10  
11  
12 (25) Samuelsson, J.; Jonsson, M.; Brinck, T.; Johansson, M. *J. Polymer Sci. Part A: Polymer*  
13 *Chem.* **2004**, *42*, 6346.  
14  
15  
16  
17 (26) Schöneich, C.; Asmus, K. D.; Dillinger, U.; Vonbruchhausen, F. *Biochem. Biophys. Res.*  
18 *Commun.* **1989**, *161*, 113.  
19  
20  
21  
22 (27) D'Aquino, M.; Dunster, C.; Willson, R. L. *Biochem. Biophys. Res. Commun.* **1989**, *161*,  
23 1199.  
24  
25  
26  
27 (28) Schöneich, C.; Dillinger, U.; von Bruchhausen, F.; Asmus, K.-D. *Arch. Biochem. Biophys.*  
28 **1992**, *292*, 456.  
29  
30  
31  
32 (29) It has been reported that the trans isomers of linoleate moieties represent the fate of the  
33 pentadienyl radical, which reacts with thiols in different conformations, see: (a) Schwinn, J.;  
34 Sprinz, H.; Droessler, K.; Leistner, S.; Brede, O. *Int. J. Radiat. Biol.* **1998**, *74*, 359. The same  
35 group later revised their conclusions in accordance with Schemes 1 and 2, see (b) Sprinz, H.;  
36 Schwinn, J.; Naumov, S.; Brede, O. *Biochem. Biophys. Acta* **2000**, *1483*, 91.  
37  
38  
39  
40  
41  
42  
43 (30) Chatgialloglu, C. *Helv. Chim. Acta* **2006**, *89*, 2387  
44  
45  
46 (31) See Supporting Information.  
47  
48  
49 (32) Ross, A. B.; Mallard, W. G.; Helman, W. P.; Buxton, G. V.; Huie, R. E.; Neta, P. *NDRL-*  
50 *NIST Solution Kinetic Database – Ver. 3*, Notre Dame Radiation Laboratory, Notre Dame, IN  
51 and NIST Standard Reference Data, Gaithersburg, MD (1998).  
52  
53  
54  
55  
56  
57  
58  
59  
60

- 1  
2  
3 (33) Based on the  $G(e_{aq}^-, HO^{\bullet}, H^{\bullet}) = 0.61 \text{ mmol J}^{-1}$  in water and  $G(HOCH_2^{\bullet}) = 0.67 \text{ mmol J}^{-1}$  in  
4 methanol, see: Spinks, J. W. T.; Woods, R. J. *An Introduction to Radiation Chemistry*, 3<sup>rd</sup> ed.;  
5 Wiley: New York, 1990; p 421.  
6  
7  
8  
9  
10 (34) Wayne Moss, C.; Lambert-Fair, M. A. *J. Clin. Microbiol.* **1989**, 1467.  
11  
12 (35) Mejanelle, L.; Laureillard, J.; Saliot, A. *J. Microbiol. Methods* **2002**, 40, 221.  
13  
14 (36) (a) Patterson, L. K.; Hasegawa, K. *Ber. Bunsenges. Phys. Chem.* **1978**, 82, 951. (b)  
15 Heijman, M. G.; Heitzman, A. J. P.; Nauta, H.; Levine, Y. K. *Radiat. Phys. Chem.* **1985**, 26, 83.  
16  
17 (37) Small, R. D.; Scaiano, J. C.; Patterson, L. K. *Photochem. Photobiol.* **1979**, 29, 49.  
18  
19 (38) (a) Calvert, J. G.; Pitts, J. N., Jr. *Photochemistry*; Wiley: New York, 1965; pp. 488–492. (b)  
20 Knight, A. R. In *The Chemistry of Thiol Group, Part 1*; Patai S., Ed.; Wiley: London, 1974; pp.  
21 455–479.  
22  
23 (39) Wong, P. C.; Griller, D.; Scaiano, J. C. *J. Am. Chem. Soc.* **1982**, 104, 5106.  
24  
25 (40) Paul, H.; Small, R. D.; Scaiano, J. C. *J. Am. Chem. Soc.* **1978**, 100, 4520.  
26  
27 (41) BB1K/ 6-31+G\*\* calculations on *Z*- and *E*-isomers of 2-butene predict rate constants  $k_Z^a =$   
28  $1.8 \times 10^4 \text{ M}^{-1} \text{ s}^{-1}$ ,  $k_E^a = 1.7 \times 10^4 \text{ M}^{-1} \text{ s}^{-1}$ . Note that the values reported in ref 18 should be  
29 multiplied by the molar volume ( $24.1 \text{ L mol}^{-1}$ ) at 20° C and 1 atm.  
30  
31 (42) BB1K/ 6-31+G\*\* calculations on *Z*- and *E*-isomers of 2-butene predict rate constants  $k_Z^f =$   
32  $6.4 \times 10^5 \text{ s}^{-1}$  and  $k_E^f = 3.3 \times 10^7 \text{ s}^{-1}$ .  
33  
34 (43) DeZutter, C. B.; Horner, J. H.; Newcomb, M. *J. Phys. Chem. A* **2008**, 112, 1891.  
35  
36 (44) Chatgialaloglu, C.; Zambonin, L.; Altieri, A.; Ferreri, C; Mulazzani, Q. G.; Landi, L.; *Free*  
37 *Radic. Biol. Med.* **2002**, 33, 1692.  
38  
39 (45) Biomimetic chemistry on the protection of cis phospholipid from the thiyl radical  
40 isomerization by active species like vitamins A, C and E and carotenes has been recently  
41  
42  
43  
44  
45  
46  
47  
48  
49  
50  
51  
52  
53  
54  
55  
56  
57  
58  
59  
60

1  
2  
3 reported: (a) Lykakis, I. N.; Ferreri, C.; Chatgililoglu, C. *Arkivoc* **2015**, 140; (b) Chatgililoglu,  
4  
5 C.; Ferreri, C.; Lykakis, I. N.; Mihaljević, B. *Isr. J. Chem.* **2014**, *54*, 242.  
6  
7

8 (46) Jacobine, A. F. Thiol-ene photopolymers. *Radiation Curing in Polymer Science and*  
9  
10 *Technology* **1993**, *3*, 219-268.  
11

12 (47) Wardman, P. In *S-Centered Radicals*; Alfassi, Z. B., Ed.; Wiley: Chichester, 1999; pp  
13  
14 289–309.  
15  
16  
17  
18  
19  
20  
21  
22  
23  
24  
25  
26  
27  
28  
29  
30  
31  
32  
33  
34  
35  
36  
37  
38  
39  
40  
41  
42  
43  
44  
45  
46  
47  
48  
49  
50  
51  
52  
53  
54  
55  
56  
57  
58  
59  
60

